



Multibeam sonar backscatter data processing

Alexandre C. G. Schimel^{1,2} · Jonathan Beaudoin³ · Iain M. Parnum⁴ · Tim Le Bas⁵ · Val Schmidt⁶ · Gordon Keith⁷ · Daniel Ierodiaconou²

Received: 14 June 2017 / Accepted: 12 January 2018 / Published online: 31 January 2018
© Springer Science+Business Media B.V., part of Springer Nature 2018

Abstract

Multibeam sonar systems now routinely record seafloor backscatter data, which are processed into backscatter mosaics and angular responses, both of which can assist in identifying seafloor types and morphology. Those data products are obtained from the multibeam sonar raw data files through a sequence of data processing stages that follows a basic plan, but the implementation of which varies greatly between sonar systems and software. In this article, we provide a comprehensive review of this backscatter data processing chain, with a focus on the variability in the possible implementation of each processing stage. Our objective for undertaking this task is twofold: (1) to provide an overview of backscatter data processing for the consideration of the general user and (2) to provide suggestions to multibeam sonar manufacturers, software providers and the operators of these systems and software for eventually reducing the lack of control, uncertainty and variability associated with current data processing implementations and the resulting backscatter data products. One such suggestion is the adoption of a nomenclature for increasingly refined levels of processing, akin to the nomenclature adopted for satellite remote-sensing data deliverables.

Keywords Multi-beam · Echosounder · Echo-sounder · Backscatter mosaic · Angular response · Backscatter · Seafloor characterization

Introduction

Originally designed to measure seafloor bathymetry, multi-beam sonar systems now routinely record seafloor backscatter data, which are commonly processed into a backscatter mosaic and less commonly into a set of angular responses (Lurton and Lamarche 2015). A *backscatter mosaic* is the common term for a georeferenced image—usually represented in gray scale—of the seafloor acoustic backscattering strength (or related variable) (Fig. 1a), while an *angular response* is the common term describing the variation of the seafloor acoustic backscattering strength (or related variable) with the angle of incidence of the acoustic signal at the seafloor (Fig. 1b). Angular responses are typically calculated for a single ping, a set of consecutive pings, or a given geographical area, and are typically represented as a mean value for each angle (“angular response curve”) as in Fig. 1b, or a color-coded distribution of values for each angle (“angular response 2D histogram”, see Le Gonidec et al. (2003) for examples). The motivation for producing those two outputs is the identification of different seafloor types and morphology, which show as regions of different levels

✉ Alexandre C. G. Schimel
alex.schimel@gmail.com

¹ National Institute of Water and Atmospheric Research (NIWA), Taihoro Nukurangi, 301 Evans Bay Parade, Hataitai, Wellington 6021, New Zealand
² Deakin University, School of Life and Environmental Sciences, Centre for Integrative Ecology (Warrnambool Campus), Princes Hwy, Sherwood Park, PO Box 423, Warrnambool, VIC 3280, Australia
³ Quality Positioning Services Canada Inc, Fredericton, Canada
⁴ Centre for Marine Science and Technology, Curtin University, Bentley, WA, Australia
⁵ National Oceanography Center Southampton, European Way, Southampton SO14 3ZH, UK
⁶ Center for Coastal and Ocean Mapping, University of New Hampshire, 24 Colovos Road, Durham, NH, USA
⁷ CSIRO Oceans & Atmosphere, Hobart, TAS, Australia

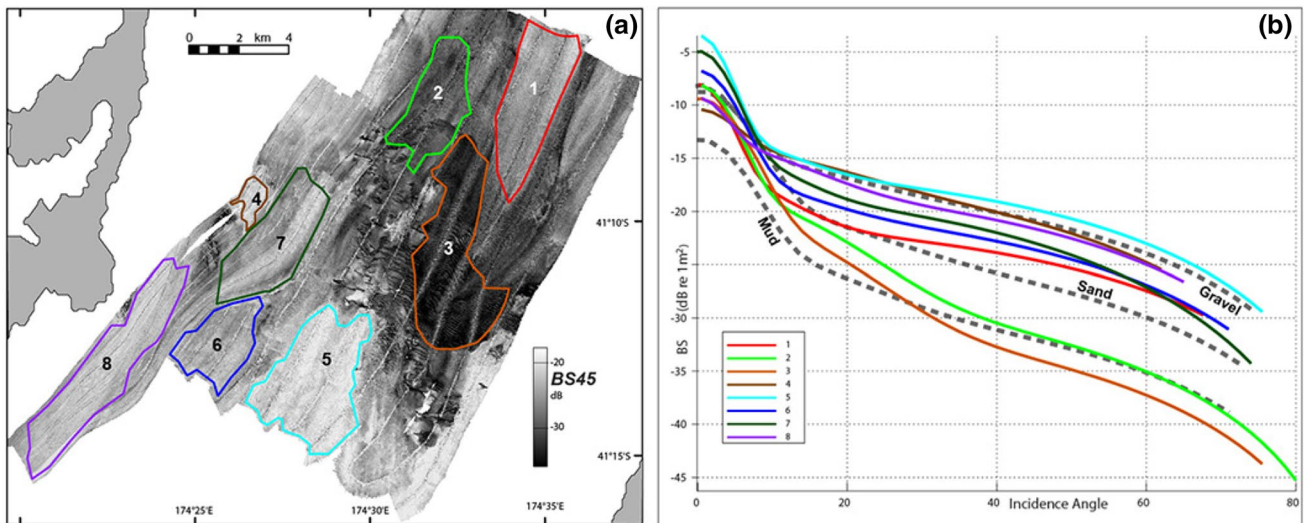
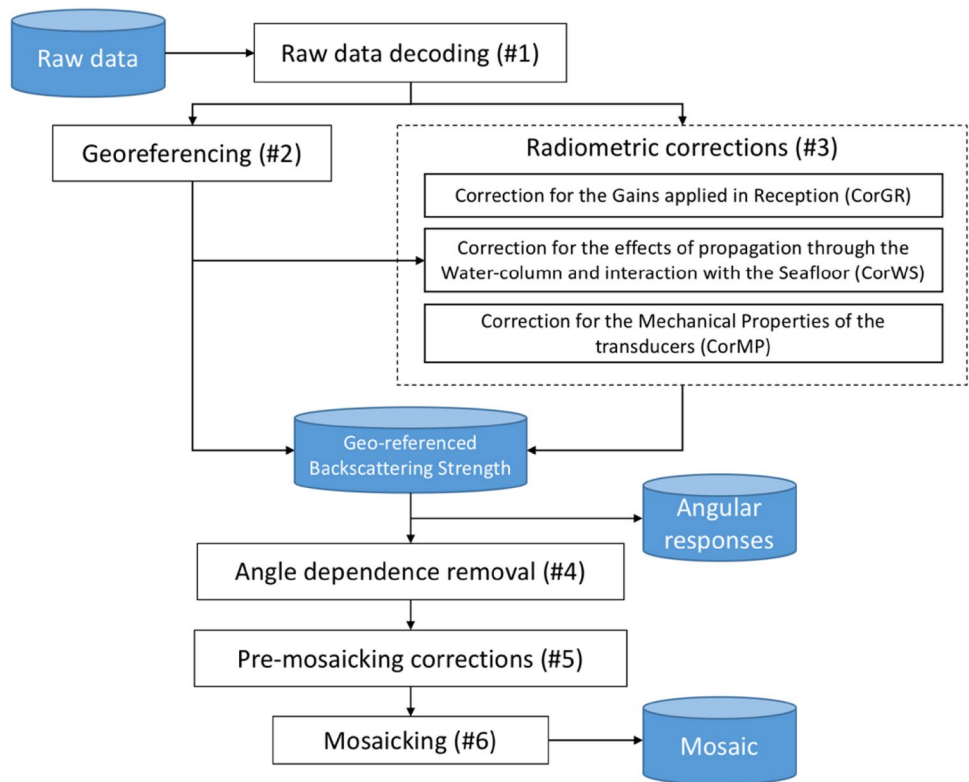


Fig. 1 Example of a backscatterer mosaic (a) and corresponding angular response curves (b). Data shown are a subset of a Kongsberg Maritime EM300 dataset (30 kHz) acquired in the Narrows Basin, Cook Strait, New Zealand, and processed using the IFREMER SonarScope software. The coloured angular response curves represent the mean

backscatter level computed from the areas defined by polygons on the backscatterer mosaic. The angular response curves in dashed lines are results from a geophysical model for some typical seabed types. Figures modified from Lamarche et al. (2011)

Fig. 2 The backscatter data processing chain



and/or textures on a backscatter mosaic, and different shapes in angular responses curves or 2D histograms.

Backscatter mosaics and angular responses are obtained from the multibeam sonar raw data files through a series of

data processing stages (Fig. 2). However, the implementation of these stages tends to differ—whether in order, level of detail, or methodology—between multibeam sonar manufacturers, between models from the same manufacturer,

between operation modes of the same sonar system, between data processing software, and between software versions. This variability in approaches to implementation and the lack of control on some of these processing stages has resulted in a general inconsistency in the backscatter mosaics and the angular responses being produced to date (Lucieer et al. 2017).

This article provides an overview of backscatter data processing, including discussions on the possible levels of detail, algorithms, and alternative approaches to implementation. Our objectives are (1) to provide the general user of backscatter mosaics and angular responses with an understanding of the acoustic principles, processing techniques, and levels of freedom that characterize the processing that generates those data products; and (2) to provide the manufacturers of multibeam sonar systems (henceforth “manufacturers”), the manufacturers of backscatter data processing software (henceforth “programmers”), and the users of these systems and software (henceforth “operators”) with an awareness of the sources of inconsistency in backscatter data products, which tend to restrict the benefits that these products provide to their users. Based on our review of the processing chain, we propose a possible common terminology and nomenclature, as well as a set of recommendations to manufacturers, programmers and operators in order to assist reducing this inconsistency in the future.

Stage 1: Raw data decoding

The very first processing stage is the necessary decoding of the backscatter data values (and other required information) recorded in the raw data files. These data are encoded in a binary format that is proprietary to each manufacturer and described in detail in manufacturer documentation. However, the lack of standard encoding format implies that backscatter data representation (i.e. its units and semantic meaning) typically varies across manufacturers. Moreover, this representation has continuously evolved with hardware and software updates, resulting in variation for a same manufacturer across sonar models or firmware versions.

For most manufacturers, backscatter data now exist in several types, with the most common ones being the “single value per beam” and the “beam time-series” types. In the “single value per beam” type, the value recorded may be the backscatter amplitude of the sample corresponding to the bottom detection, or may be calculated from nearby samples (such as the average amplitude of the samples corresponding to the beam footprint). The “beam time-series” type consists in a short sequence of backscatter samples for each beam, usually selected by the firmware as the range of samples theoretically corresponding to the propagation of the pulse over the seafloor. Another common data type is the

“half-swath time-series” type, which consists in one uninterrupted time-series for each side of the swath, and is meant to emulate a sidescan sonar trace. Finally, backscatter data can also come as a “time-series of amplitudes and angles” format, which is the native output of phase-measuring bathymetric sidescan sonars. Data in this format can be found in full resolution and sometimes averaged/decimated. Note that given the absence of accepted standard or accurate academic definition, the terminology for each of these data types vary between manufacturers; for example, the “single value per beam” type is found as “Beam Intensity” in Kongsberg Maritime systems, “Bathy Intensity” in R2Sonic systems, or “Beam magnitude” in Teledyne RESON systems, while the “beam time-series” type is found as “Seabed Image” (Kongsberg Maritime) or “Snippets” (R2Sonic and Teledyne RESON).

For any given manufacturer, the representation of each data type may be dependent on the version of the sonar system and acquisition software. For example, backscatter data in Kongsberg Maritime systems are found at a 0.1 dB resolution in newer models, but used to be recorded at a 0.5 dB resolution in older systems. It can also be expected that manufacturers upgrade the algorithm implemented by the firmware to calculate a given data type over time. It is therefore important for manufacturers to always specify unambiguously the data types and versions that were recorded in the raw data files. This is necessary for programmers to use decoding adapted to each specific data type and version, and for operators to select the data type appropriate to their needs and annotate output products with this information. Knowledge of the exact source of the data at the origin of final backscatter data products is essential for within-system data normalization.

Stage 2: Georeferencing

The second processing stage is the calculation of the geographical location of each sample in the backscatter dataset (i.e. “georeferencing”). This is aided by the fact that data files produced by multibeam sonar systems and their ancillary sensors contain all the necessary information for such calculation, including the position and attitude of the vessel in the geographical frame, location and setup of the sonar head in the vessel frame, geometry of the beams, and sound velocity in the water column. Moreover, software for the processing of multibeam bathymetry data already implement detailed algorithms that use this information to calculate the precise geographical location of the sample in each beam that corresponds to the seafloor.

Thus, if the backscatter data can be unambiguously associated with the bottom detect of each beam (i.e. the “single value per beam” data type), then the standard bathymetry

data processing directly provides georeferencing for the backscatter data as well. For other backscatter data types, additional processing is required to complete this georeferencing stage, often drawing from “geometric corrections” methodologies originally designed for data from sidescan sonar systems (Beaudoin et al. 2002; Le Bas and Huvenne 2008).

Backscatter data in the “half-swath time-series” format can be georeferenced using the same type of slant-range corrections designed for sidescan sonar imagery, using a flat seafloor assumption. However, the bathymetry data provided in each beam makes it possible to improve significantly on that basic procedure by precisely locating the trace on the ground along the swath (Beaudoin et al. 2002).

Backscatter data in the “beam time-series” format can be georeferenced using methodologies derived from the approaches discussed above. One method is to use the bathymetry information of the bottom detect in the beam to georeference the corresponding sample in the time series—as if it were in the “single-value-per-beam” format—and then to georeference the other samples by interpolating the bathymetry between neighboring beams. Another common method is to transform these beam time-series data into half-swath time-series and apply the georeferencing methodology specific to that format. Such format transformation is particularly relevant for beam time-series that have been formed specifically as to create a continuous trace along the seafloor when concatenated. For beam time-series that have been formed specifically to cover the beam footprint, one can average samples between beams with overlapping footprint so as to eventually form a continuous half-swath trace (Augustin et al. 1994; Beaudoin et al. 2002).

Stage 3: Radiometric corrections

The third processing stage consists of adjustments to the recorded backscatter level to produce a level free of undesirable dependencies. In effect, the signal level recorded in the raw data files is usually not directly exploitable, as the original transmitted sound pulse was considerably modified by its interaction with the water-column, the seafloor, and the sonar system receive hardware and software. The most desirable backscatter level is the physically meaningful backscattering strength $BS_f(\beta)$ (in dB re 1 m² per m²), which is only dependent on the system frequency f , the angle of incidence on the seafloor β , and the morphology and composition of the seafloor that scattered the signal (Lurton 2010). In practice however, the backscatter level recorded in the files is (in dB re 1 V):

$$BL_0 = SL - 2TL + TS + SH + PG \quad (1)$$

where SL is the source level in the acoustic axis (in dB re 1 μ Pa at 1 m), TL is the one-way transmission loss (in dB), TS is the target strength of the seafloor that contributed to the return signal (in dB re 1 m²) (MacLennan et al. 2002), SH is the sensitivity of the receive array (in dB re 1 V/ μ Pa), and PG is the gain introduced by the electronics from signal reception to recording in data files (in dB) [adapted from Augustin and Lurton (2005)].

Backscattering strength is derived from Target Strength but this task is not straightforward as the Target Strength is the total contribution over the total insonified area A of the backscattering cross-section bs_f (in natural values, with $BS_f = 10\log_{10}bs_f$) occurring over area element dA and modulated by the directivity patterns in transmission and reception bp_T and bp_R , which both depend on the transmission angles θ [adapted from Hellequin et al. (1997)]:

$$TS = 10\log_{10} \int_A bs_f(\beta) \cdot bp_T(\theta) \cdot bp_R(\theta) dA \quad (2)$$

In practice, the common approximation is to consider instead:

$$TS = BS_f(\beta) + 10\log_{10}A \quad (3)$$

And add the directivity patterns to the full equation for the recorded level, that is (Augustin and Lurton 2005):

$$BL_0 = SL + BP_T(\theta) - 2TL + BS_f(\beta) + 10\log_{10}A + SH + BP_R(\theta) + PG \quad (4)$$

where BP_T and BP_R are the directivity modulations (i.e. beam patterns) in transmission and reception, respectively (in dB).

This latest equation allows retrieving $BS_f(\beta)$ from the recorded level BL_0 and the process of doing so is often termed “radiometric corrections”. In practice, most software implementations consist in one single operation accounting for all necessary corrections. Here we will distinguish these corrections in three themes: a Correction for the Gains applied in Reception (CorGR), a Correction for the effects of propagation through the Water-column and interaction with the Seafloor (CorWS), and a Correction for the Mechanical Properties of the transducers (CorMP).

Correction for the gains applied in reception (CorGR)

CorGR is the compensation of the backscatter level for all analog and digital modifications that were applied to the received signal by the hardware between the reception of the signal and its recording in the raw data files. Written collectively as PG in Eqs. (1) and (4), these modifications include analog and/or digital, static and/or time-varying

gains, as well as the effects on the signal level from the analog-to-digital conversion, beamforming, array shading and other signal processing (Beaudoin et al. 2002; Lurton 2010; Parnum and Gavrilov 2011a).

Analog gains are usually designed to increase with time of reception in order to overcome the decaying of signal strength with time/range and keep the signal at the input of the analog/digital converter within its dynamic range. Since this decay is due to phenomena represented in the sonar equation (most importantly, transmission losses TL), such time-varying gain (TVG) can be viewed as a desirable radiometric correction. Likewise, the flexibility of digital gains after analog/digital conversion makes them an attractive solution for manufacturers to finalize the radiometric correction initiated by the analog TVG. This potential of using gains for radiometric corrections and the lack of guidelines or standards in implementation resulted in a wide variability in the gain designs among sonar manufacturers, sonar models and even individual sonar systems.

At one end of the spectrum, the simplest gain implementation will take the general form:

$$PG(t) = K_1 \log_{10}(t) + K_2 \cdot t + K_3 \tag{5}$$

where t is the time of reception and K_1 , and K_2, K_3 are constant terms that are either permanently set by the hardware or modifiable by operators during the survey through the data acquisition software.

At the other end of the spectrum, the most complex gain implementations operate a full radiometric correction including—for example in Kongsberg Maritime systems—a

piecewise TVG to correct for transmission losses, area of insonification and even the seafloor angular dependence (Hammerstad 2000). Such a complex gain depends on many parameters that vary between modes of operation (pulse length), pings, transmit sectors (frequency) and receive beams (beam width), and relies on accurate parameters of the environment (absorption coefficient). Systems that implement such complex TVG have the advantage of proposing in their data files a level BL_0 that approximates the desired BS . However, their main inconvenience is that the complexity of such TVG makes its compensation more difficult. Given that it is almost always possible to implement more accurate radiometric corrections in post-processing, such compensation is often desirable (Fig. 3).

The signal processing in reception introduces other gains than the TVG discussed above. For example, the modern use of frequency-modulated (FM) and amplitude-shaded pulses to increase signal-to-noise ratio requires a matched-filter processing (“pulse compression”), which introduces a shift in the amplitude of the signal, that is, a gain in reception. This gain often goes unreported and it is often unsure whether the firmware of the various systems automatically compensates for it and, in case they do, if it is done appropriately.

Thus, it is almost always better to remove the gains from the recorded data, whatever their level of complexity. Such compensation should theoretically be unambiguous since all these processes are analogically defined in the hardware, digitally hard-coded in the firmware, or set by the operators in the acquisition software. However, the information

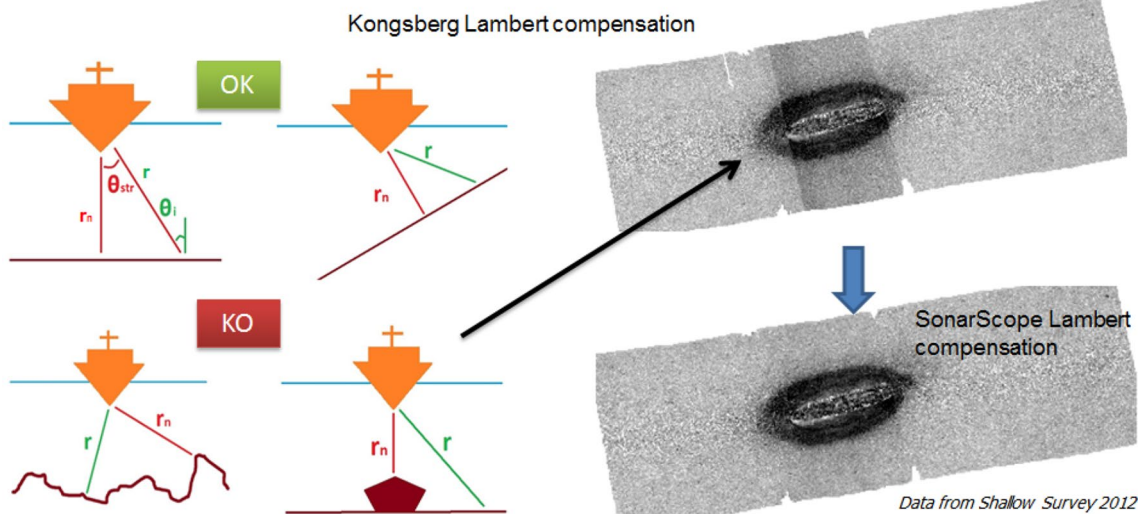


Fig. 3 Example of backscatter mosaic artefact induced by maladapted gains, and compensated in post-processing. Here, the dynamic gain implemented in a Kongsberg Maritime system was designed to correct for insonified area but fails to account for the complex bathymetry induced by a shipwreck lying on a flat seafloor. Correcting the

artefact required the complete removal of the gain, followed by a more appropriate compensation of insonified area in post-processing [from Augustin et al. (2013). Data courtesy of Shallow Survey 2012, processed with SonarScope]

is not always made available to the operator in the data files or clearly described in metadata or documentation. Even in the best-case scenario of properly documented gain designs, their analog nature makes them prone to difference between design and hardware implementation, and change over time due to the ageing of components.

A potential solution is to empirically measure the gain under all possible combinations of modes of operations and parameter settings [see for example Rice et al. (2012)]. In this context, it would make sense that in the future manufacturers would seek to minimize the complexity of gains to help reducing errors in their subsequent compensation (a possible development aided by the increasing dynamic range of modern analog/digital converters), include all necessary design details in documentation, implement a method of empirical measurement at all gain stages (with a test signal perhaps), and either record those measurements in the data files or offer an accommodation in processing software for these measurements.

If these gains are removed successfully, the resulting corrected backscatter level is the level received at the transducer face prior to application of gain, commonly referred to as Received Level (Lurton 2010) and noted here BL_1 (in dB re 1 V):

$$BL_1 = BL_0 - PG = SL + BP_T(\theta) - 2TL + BS_f(\beta) + 10\log_{10}A + SH + BP_R(\theta) \quad (6)$$

Correction for the effects of propagation through the water-column and interaction with the seafloor (CorWS)

CorWS is the compensation of the backscatter level for the predictable effects of the physical interaction of the sound pulse with its environment, namely: the transmission losses in the water column, and the area insonified by the pulse within the beam width on the seafloor at the moment of interaction. Backscatter data processing software suites implement these two compensations using different algorithms whose level of detail operates a trade-off between realism/accuracy and speed/simplicity. The levels of detail that are implemented to date are often following common practices that might have been devised at times where correction complexity was limited by computer processing power. The recent increase in computer processing power has resulted in increasingly more realistic corrections.

Transmission loss is most often modeled as a loss through geometrical spreading and a loss through absorption in the water medium, both dependent on the range R (in m):

$$R = ct/2 \quad (7)$$

$$TL = 20\log_{10}(R) + \alpha R \quad (8)$$

Where c is the velocity of sound (in m/s), t is the time of reception (in s), and α is the absorption coefficient (in dB/m, although typically reported in dB/km).

The velocity of sound and the absorption coefficient depend on temperature, salinity, pressure and pH, and thus tend to vary with geographical location (e.g. proximity of a zone of fresh water), time (e.g. seasons) and depth. With accurate (location and time-wise) measurement of sound velocity through depth, realistic estimates of range and corresponding depth can be obtained for each time sample. Then, with accurate estimates of absorption through depth, cumulative absorption may be calculated through the path of the signal (Carvalho and Hughes Clarke 2012). Measurements of sound velocity as a function of depth in several locations and times are often available because the frequent capture of sound velocity profiles is part of every multibeam sonar survey procedure. However, equivalent measurement is often missing for the absorption coefficient, despite its important influence on the backscatter level (Hughes Clarke 2012). Depth-dependent absorption coefficients could be estimated from profiles of conductivity, salinity and temperature taken during survey (and temperature profile are often an additional output of sound velocity profiles) or oceanography databases, using the equations in Francois and Garrison (1982). However, the approximation of absorption losses through the use of a single constant coefficient (usually calculated for an average depth) is still commonplace to date.

More so than depth, absorption coefficients are also strongly dependent on the signal frequency. This is especially relevant since modern multibeam sonar systems are increasingly designed to implement variable operating frequencies between different files, pings or transmit sectors. The TVG implemented in modern Kongsberg Maritime systems includes a modelling of absorption losses that take into account both variations in frequency and cumulative absorption through a depth-dependent coefficient. This methodology, described by Carvalho and Hughes Clarke (2012), should be adopted in post-processing for optimal correction of absorption losses.

The compensation for insonified area only requires the estimation of the total area of seafloor insonified by the pulse for each time sample t in the return signal. Theoretically, this area is defined by the pulse footprint on the seafloor at time $t/2$, which is an annulus, modulated in space by the transmit and receive beam patterns. There is considerable variation in the level of realism of such a calculation (Schimel et al. 2015).

The simplest approximation is to consider a flat seafloor and an area being the product of the instantaneous footprints in the across-track and along-track directions, which are limited by the beam width in the along-track direction and in the across-track direction for beams with near-normal

incidence, and by the pulse width in the across-track direction for beams with grazing incidence (Lurton 2010). A more realistic approximation is to also consider the seafloor slope, either estimated from the soundings in nearby beams and pings, or estimated from a model of bathymetry (Parnum 2007). Finally, the most realistic approach is to consider the full 3D vector at transmission, modulated by the vessel movement, its full refraction in the water-column, and the 3D normal vector to the seafloor at the location of interaction (Beaudoin et al. 2004).

Irrespective of the level of realism, these corrections are strongly dependent on the effective pulse length (or equivalent bandwidth) and the transmit/receive beam widths. While nominal values are available from the manufacturer and usually stored in the raw data files, the estimates necessary for an accurate correction may be very different in practice (Hughes Clarke 2012). Particularly, the pulse length is strongly affected by pulse tapering and sampling, as well as the transfer function of the transducer, and it is often unknown whether the pulse length value reported in the data is a theoretical value or an effective one considering all these effects. The use of the theoretical pulse length instead of the effective one introduces a bias depending on the magnitude of the difference; for instance, $10\log_{10}(0.5) \sim -3\text{dB}$ if the effective length is half of the theoretical one. Transmit and receive beam widths may also be very different than the nominal values. Particularly, beam width typically varies with frequency, which is very relevant for multi-sector systems.

Ideally, if the gains in reception were accurately removed from the recorded level and the transmission losses and insonified area were appropriately compensated, the resulting level, noted here BL_2 (in dB re 1 V), should only be dependent on the seafloor backscattering strength and the mechanical characteristics of the transducer in transmission and reception:

$$BL_2 = BL_1 - [-2TL + 10\log_{10}A] = SL + BP_T(\theta) + BS_f(\beta) + SH + BP_R(\theta) \quad (9)$$

Correction for the mechanical properties of the transducers (CorMP)

CorMP is the compensation of the backscatter level for the mechanical characteristics of the transducer, that is, at transmission, the transmit power in the acoustic axis modulated by the transmit beam pattern, and at reception, the efficiency of the acoustic-electric conversion of the receive array, modulated by the receive beam pattern. These are respectively represented by the terms SL , $BP_T(\theta)$, SH and $BP_R(\theta)$ in Eqs. (4, 6 and 9).

Information about source level is usually available. Because of this, it is often compensated in data processing

software at an early stage of radiometric corrections, usually along with the gains in reception. Manufacturers often list a nominal source level for different sonar models or modes of operation [see for example Hammerstad (2005) for Kongsberg Maritime systems], and the data acquisition software sometimes allow the operator to select the source level (or transmit power) and record the information in the raw data files. Information is much scarcer for the other terms. A combined transmit/receive beam pattern obtained from the testing of a prototype in a tank is sometimes provided (usually upon request). As for receive array sensitivity, this information is almost never available or requested.

However, the accuracy of this information is usually limited. Discrepancies between the design (and reporting) of a source level and its implementation are common and necessitate measurement and correction (Rice et al. 2012). Likewise, the combined beam patterns obtained from a prototype are usually different from that of individual systems as their construction, housing, and electronic components may differ from the model design (Hughes Clarke et al. 2008). In any case, system components experience degradation through time, which can affect all of these terms significantly (Hughes Clarke et al. 2008). Ideally, these terms would therefore be measured for each system and each mode of operation, before its first use and through its life cycle. The operation of measuring the combined effect of SL (or its residual after compensation of the nominal value), $BP_T(\theta)$, SH and $BP_R(\theta)$ is often called “calibration” and its result a “beam pattern”.

There are standard calibration protocols for sonar systems, usually using a solid sphere of known target strength (Demer et al. 2015). These protocols are widely used for fisheries single-beam and split-beam echosounders for example, but are much more difficult to apply to multi-beam echosounders because of their large angular swath, small individual beams and usually large number of modes of operation. Nonetheless, procedures for the calibration of multibeam echosounders in a tank have been proposed using standard spheres (Melvin et al. 2003; Foote et al. 2005; Lanzoni and Weber 2011) or extended surface targets (Heaton et al. 2017). Such procedures can readily provide the initial calibration of a system before its delivery to a client. At present however, manufacturers do not systematically perform such initial calibration for each system they produce.

Several techniques have been devised to calibrate multi-beam sonar systems in the field, with the main problem to be tackled being that the variation of seafloor backscattering strength with angle of incidence confounds the measurement of beam patterns, which vary with the transmit/receive angle. The most common solution consists of acquiring data over a seafloor of homogeneous type, fitting the data with

an appropriate *BS* model, and extracting the residual as the desired “beam pattern” (Augustin and Lurton 2005; Fonseca et al. 2006; Hughes Clarke 2015). Figure 4 illustrates the process devised by Augustin and Lurton (2005) for a multi-sector system. The result is typically checked for consistency between several different seafloor types. Beam patterns have also been extracted from large amounts of data spanning several seabed types and seabed morphology, without a need for a prior correction for a model *BS* (de Moustier and Kraft 2013). A different methodology

has been recently devised, using a dataset containing significant roll movement (Tamsett and Hogarth 2016; Hiroji et al. 2016; Hiroji and Hughes Clarke 2017). Under such conditions, a given small area of homogenous seafloor would be insonified from the same grazing angle at seafloor but different angles at transmission/reception, thus resulting in a small dataset in which the signal only varies with transmit/receive angle, giving away the beam pattern. Such beam pattern would only be derived over the small angular range provided by the roll movement, but it could then be

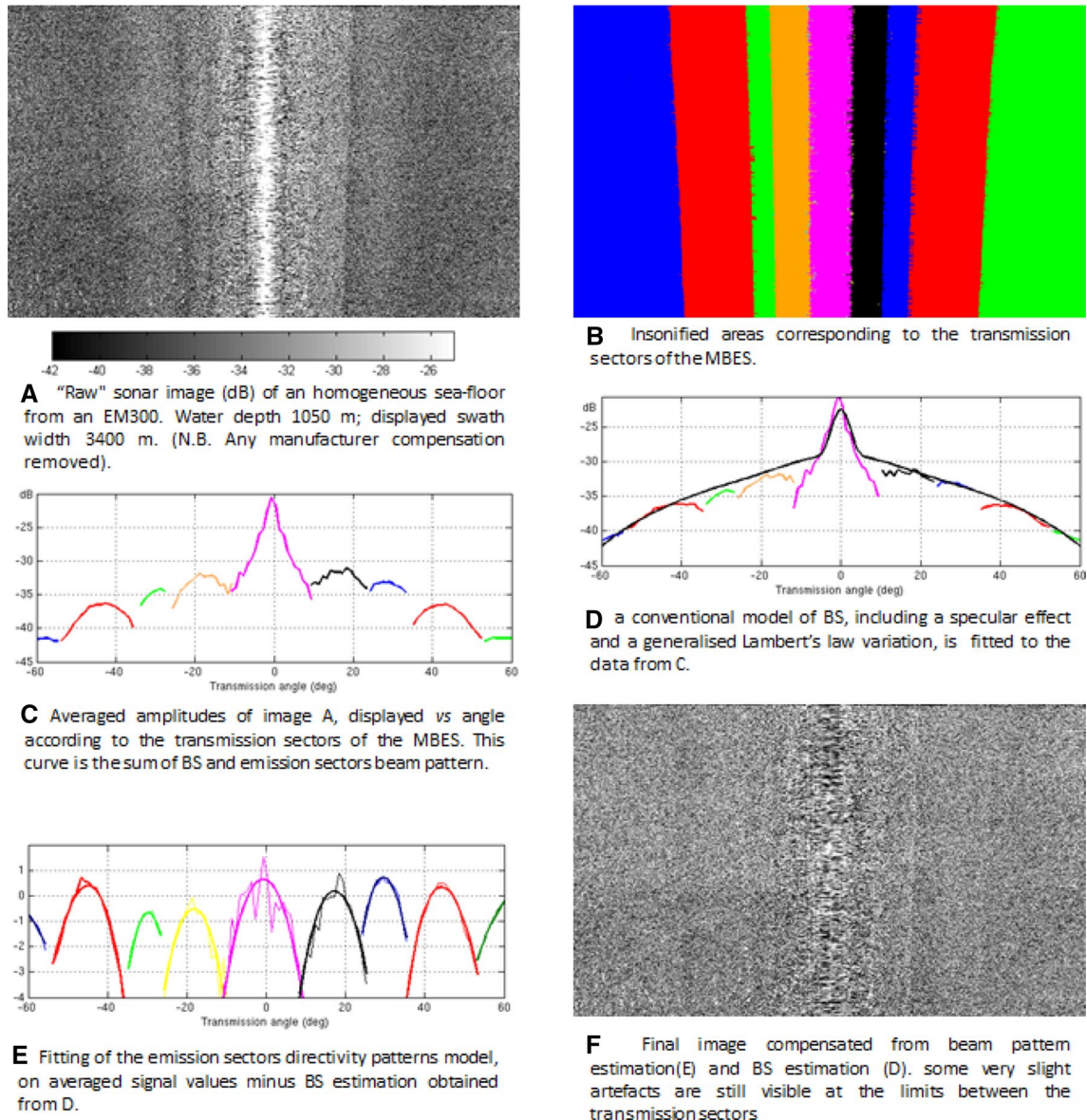


Fig. 4 Example of a methodology to measure on the field the combined effect of beam patterns in transmission and reception, for individual transmit sectors. From a Kongsberg Maritime EM300 multi-beam sonar backscatter dataset showing the effects of uncorrected beam patterns (a) and the corresponding transmit sector extent (b), the average backscatter level is calculated as a function of transmis-

sion angle (c). An appropriate physical model of *BS* is fitted to the data (d), leaving only the beam patterns. Those patterns are modelled by individual transmit sectors (e) to be used in further radiometric corrections. Applying those beam patterns as part of the radiometric corrections remove the artefacts seen previously (f). From Augustin and Lurton (2005). Data processed with SonarScope

combined with other pieces of the beam pattern obtained by applying the methodology at the same time for all patches of seafloor across the swath, thus allowing the extraction of a full beam pattern without a need to compensate for the seafloor backscattering strength.

Note that roll/pitch/yaw stabilization in modern multi-beam sonar systems affect beam patterns. For systems without stabilization, the beam patterns may be measured at angles relative to the sonar acoustic axis. For systems with stabilization, the beam patterns may be measured at angles relative to the vertical, within the limits of the stabilization capabilities of the system.

Most processing software can implement a correction for beam patterns, using calibration functionalities that implement one of the methods discussed above to retrieve empirical estimates of the combined effect of SL , SH and the beam patterns (Augustin and Lurton 2005; Leblanc and Foster 2015; QPS 2017). These procedures have the additional advantage of compensating for the constant terms in the gains in reception that may have not been properly compensated for at the first step of radiometric corrections.

The level resulting from an efficient implementation of all radiometric corrections including this last calibration step is the seafloor backscattering strength BS :

$$BL_3 = BL_2 - [SL + BP_T(\theta) + SH + BP_R(\theta)] = BS_f(\beta) \quad (10)$$

Notes on angular response analysis

$BS_f(\beta)$ is characteristic of the seafloor type and geomorphology, but also dependent on the frequency f and on the angle of incidence β . Since the frequency of the system is known and the prior radiometric corrections involved the estimation of the angle of incidence, the seafloor-characteristic angular response can thus be directly obtained at that stage of the processing. Ideally, data samples would be compiled over areas that are both (1) of assumed homogenous seafloor-type and (2) large enough to obtain a number of samples that is sufficient to overcome statistic fluctuations and covers the entire angular range. The distribution of backscattering strength over the angular range—or more commonly the mean backscattering strength per angle—can then be analyzed to characterize the seafloor at the origin of this dataset.

A large body of research has been dedicated to identifying, understanding, quantifying and modelling the several physical phenomena that are responsible for the seafloor re-emitting portions of an incident acoustic signal—specular reflection, surface scattering and volume scattering (Urick 1983; APL 1994, 2000). In theory, fitting such physical models to angular response data would allow estimating some key physical parameters of the seafloor, thus allowing its identification (e.g. Fonseca and Mayer 2007). The two main issues with this approach are that the number

of parameters in most physical models of backscattering strength is too large to invert these models efficiently and unambiguously, and that no model exists that reliably characterize a heterogeneous seafloor, of which most of the seafloor consists.

Because of these issues, angular response analyses more often consist in fitting simpler empirical models to the angular response (e.g. Hughes Clarke 1994; Hughes Clarke et al. 1997; De Falco et al. 2010; Lamarche et al. 2011; Huang et al. 2013), or using directly the angular response values at set angles as the parameters to be fed into a seafloor-type supervised-classification algorithms (e.g. Che Hasan et al. 2012). The advantage of these approaches is that they don't rely explicitly on physical meaningful variables, and are therefore unaffected by systematic bias in the data: as long as the relative level is consistent and the variation with incidence angle is only dependent on seafloor characteristics, the results will be the same. These approaches are therefore applicable even in the very common event that the systematic terms of some radiometric corrections needed for accurate reduction to BS are missing, such as static gains, source level and receive array sensitivity. In other words, if the purpose of the backscatter data processing is to produce angular responses for an empirical analysis, then the radiometric corrections in the processing chain can be simplified. However, if these systematic terms change (for instance with data acquisition settings or hardware components ageing), the parameters determined from empirical models must be re-estimated. Thus, the interest of these methodologies is usually limited to the identification of differences between seafloor types within a single survey dataset.

Note that the dependence of $BS_f(\beta)$ with frequency implies the possibility to characterize or discriminate between seafloor types also on the basis of potentially different angular responses at different frequencies. The increasing availability of systems operating at different frequencies, and the trend towards new broadband systems will likely result in backscattering strength being analyzed in the future both as a function of frequency as well as incidence angle (Hughes Clarke 2015).

Stage 4: Angle dependence removal

Stage 4 is the compensation of the backscattering strength for its dependence with angle of incidence at the seafloor. Indeed, if one were to create a mosaic with the backscattering strength retrieved after radiometric corrections, its dependence with angle would show as a strong striping oriented along the vessel track, which would hinder both visual interpretation and image processing algorithms (Fig. 5). Thus, BS is typically mosaicked only after its angular dependence has been compensated. However, such

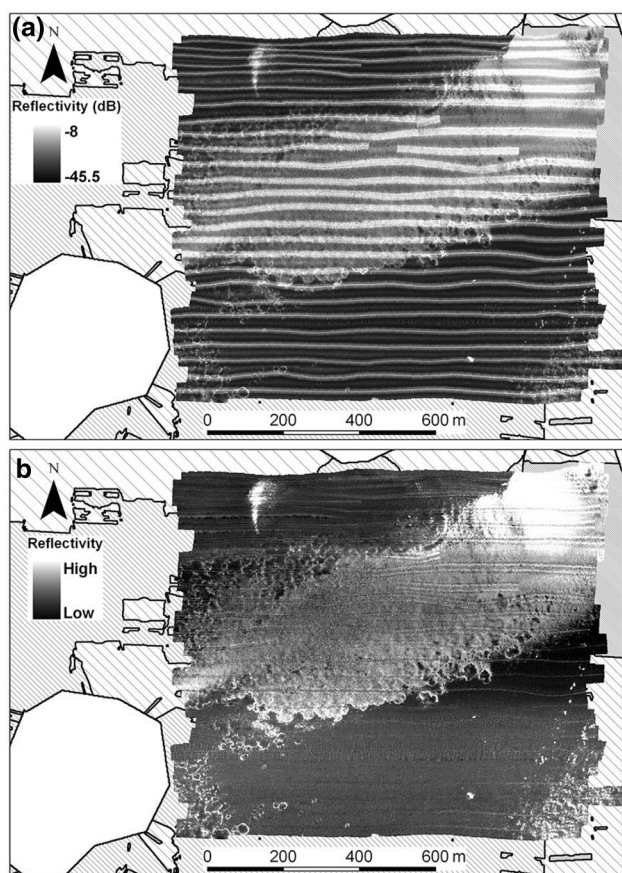


Fig. 5 Example of georeferenced and mosaicked backscatter level without (a) and with (b) correction for angular dependence. The variation with angle of incidence in the first panel shows as a strong striping along the vessel track (oriented East–West in this case). Note how the width of the striping artefact differs between strongly reflective and weakly reflective seabed types (respectively in light and dark tones), illustrating that the angular dependence itself depends on seabed type. In this example, the angular dependence was corrected by taking the beam angle as incidence angle (i.e. an assumption of a flat seafloor and neglecting vessel movements and refraction in the water column), removing the average value per angle calculated on each file, and not introducing an average level afterwards (i.e. no reference angle) Figure adapted from Schimel et al. (2010)

correction is not trivial because the fact that this angular variation is itself dependent on seafloor type and morphology implies that it cannot be ideally corrected without prior knowledge of the distribution of the different seafloor types and morphology over the dataset (Hughes Clarke 2012).

The standard technique to correct for angular dependence consists in subtracting from the backscatter level an “expected” level for the corresponding angle of each sample (which normalizes the level across angles) and adding the expected level for a “reference” angle or the average level within a “reference” angular interval (which reintroduces the difference between seafloor types). This way, the local

angle-dependent backscatter values are replaced by an angle-independent value that captures the instantaneous variation in backscatter level from the mean, scaled to the reference angle (Hughes Clarke 2012). There are two main implementation choices for this approach that dramatically affect the aspect of the subsequent mosaic: (i) the methodology used to create the “expected” curve, and (ii) the choice of the angle or angular interval used as a reference.

Generic angular responses measured for typical seafloor types, or generated from canonical physical models, such as Jackson’s (APL 1994, 2000), would be possible approaches to create the expected curve. However, in most field data, both the seafloor type and its spatial variability are a-priori unknown, making this approach inapplicable. Therefore, expected curves are most often created from the data themselves, usually by computing the average of the backscatter level over a subset of data. In this case, a trade-off controls the choice in the definition of the data subset used to create the expected curve (Hughes Clarke 2012). The larger the subset, the more likely it is to overcome the statistical variation in the data and thus smooth out across-track variations, but the more likely it is to overlap several different seafloor types and to mix up their typical angular responses, creating along-track artefacts, particularly at transition between seafloor types. Conversely, a very small subset will minimize along-track artefacts at the expense of a failure to smooth out all across-track variations. A variety of approaches have been explored in that respect. Some adopted for the creation of a single expected curve for the entire dataset, whether built from the entire dataset itself (Preston 2009) or from a carefully selected line (Beaudoin et al. 2002). More often, several curves are created based on data subsets selected according to the data to be corrected. At the most basic, one can use the data from each track line to form the curve to be used to correct the data in that same line (Schimel et al. 2010). A more common option is to form a curve from a series of consecutive pings encasing the ping to correct, resulting in a “sliding window” of corrective curves (e.g. Fonseca and Calder 2005; Gavrilov et al. 2005; Hughes Clarke et al. 2008; Kloser et al. 2010; Parnum and Gavrilov 2011b). This approach presents the advantage of allowing the operators to adjust the size of the “window” for better results. Going one step further, the early Geocoder offered a version of this approach where separate curves were created for each side of the swath independently.

The choice of the reference angle is also an important one and there is no standard in that respect either. Fonseca et al. (2009) used the relatively wide angular interval 20°–60° and that choice is still used in QPS FMGT and presumably other subsequent versions of Geocoder. The new backscatter data processing in Caris HIPS & SIPS uses 30°–60° (Leblanc and Foster 2015). Lamarche et al. (2011) suggested using

45° (effectively, the narrow interval 43°–47°) as a standard reference angle, given that it is at this angle that angular responses tend to differ the most between common seafloor types. This reference is implemented in the IFREMER software Sonarscope.

It is worth noting that there are variations on the common methodology described above. In the same manner as the average level is replaced with a reference average level, Parnum et al. (2006) and Preston (2009) have explored replacing the standard deviation of the signal by a reference standard deviation, thus completing a full signal normalization. More commonly used but less understood are the three different algorithms termed “Flat”, “Trend” and “Adaptive” of Geocoder and its subsequent versions such as QPS FMGT. While the default “Flat” is likely the standard method described previously, it is unsure what “Trend” and “Adaptive” do.

Software suites usually permit the adjustment of some parameters of their angular dependence correction algorithm, thus allowing operators to select the parameters that minimize the angular-dependent residual artefacts in their backscatter mosaics. However, information on the details of the algorithm and the parameters selected are often lacking from the data products themselves (or their metadata), even though these operational choices strongly influence the final aspect of the backscatter mosaic.

Stage 5: Pre-mosaicking corrections

The fifth processing stage consists in operations applied to the angular-dependence-corrected backscatter level aimed at enhancing the visual quality of the final image, mostly despeckling and anti-aliasing. Although many operators may prefer to apply any visual enhancement on the final product instead (that is, the backscatter mosaic), there are advantages to apply at least some visual enhancement operations before mosaicking due to the dataset still being at its full resolution at this stage.

One important operation is down-sampling the variable as data at this stage often have a much higher spatial resolution than the mosaic grid that they will be contributing to, which tends to result in aliasing. For example, data after angular dependence removal may be available at 0.05 m resolution, while the desired mosaic is to be produced at a resolution of 0.50 m. Data can thus be subsampled or averaged in bins approximating the resolution of the desired mosaic.

Another possible operation is filtering the high-frequency noise that is common in acoustic data (speckle). This “despeckling” operation usually consists in the application of a noise-reduction low-pass filter such as a median filter. Applications in two dimensions (across-track/along-track) are possible, but this operation is more often applied in one

dimension in the across-track direction as the data density is often much higher in that dimension.

Stage 6: Mosaicking

The sixth and final processing stage consists in mapping the angular-dependence-corrected (after stage 4) and possibly filtered (after stage 5) backscatter level into the georeferenced image that is the backscatter mosaic. “Backscatter mosaic” is a terminology introduced in sidescan sonar data processing, at a time when single files were processed into separate images to be combined (“mosaicked”) into one. With multibeam sonar backscatter data, one rarely produces individual images for each file; the process of creating the final image more often consists in gridding all data at once. However, the terminology has become entrenched into everyday use. Mosaicking can be broken down in a sequence of four processing steps.

The first step is the gridding itself. It is defined by the two important decisions of choosing an appropriate grid resolution and an appropriate strategy for filling this grid given the overlap of data from a variety of sources (different beams, pings, and files) with various quality. The grid resolution is more or less constrained by the overall horizontal distance between data points, which is dependent on a number of parameters of the data acquisition, survey design, but most importantly on depth, with higher data density in shallower waters. In contrast, the gridding strategy is largely a matter of choice.

A suitable grid resolution is usually the smallest grid cell size such that the final grid contains little to no gaps (that is, grid cells without data samples contributing to it). The two important factors in that decision are the spatial proximity of samples, and the spatial extent of seafloor that contributed to the signal of any given sample and can thus be attributed the value of that sample (i.e. footprint). The main issue is that proximity and footprint can differ widely between data types, across the swathe and across dimensions. In the across-track dimension, “beam time-series” data samples are much closer to each other than data samples in the form of “single value per beam”, with proximity between samples being dependent on sampling frequency in the first case and the angular interval between beams in the second case. In that latter case, a constant angular interval between beams results in data samples being much closer to each other for beams intersecting the seafloor at near normal incidence (typically, near the nadir) than for beams intersecting the seafloor at grazing angles (typically, near the edges of the swath). However, the limiting factor is often in the along-track dimension, where proximity between samples depends on vessel speed and ping rate, while footprint depends on transmit beam

width and range, irrespective of the data type. All these estimates of distance between samples will be strongly modulated by the movements of the vessel for unstabilized systems, with uncompensated pitch and yaw leading to gaps in places in the along-track direction (Hughes Clarke 2012). Finally, one must consider the increase in data density due to the use of dual head systems, or overlapping adjacent lines. In the case where data samples are much closer to each other in the across-track dimension than in the along-track dimension (typically, using beam time-series on deep water systems), it is common to choose a grid resolution that is small enough to retain the resolution of the across-track data and interpolate in the along-track direction (Augustin et al. 1994).

Gridding strategy is governed by (1) the mathematical operation used to compute the final value for a grid cell when several data points contribute to it, and (2) the management of overlapping lines. The most common gridding implementations consists in taking the mean of the backscatter values, in linear or logarithmic (dB) units. Averaging in linear units is the mathematically correct choice but it is biased towards higher values, while averaging in logarithmic units will hurt the sensibility of the more mathematically-oriented, but produce a result that is less sensitive to the higher outliers. For instance, considering a set composed of one sample showing a strong return of -20 dB and four samples at the very low return of -70 dB, an average in logarithmic units would be -60 dB, which highlights the overall trend of more low returns in the set, while an average in linear units would be a still relatively strong -33.9 dB, highlighting the bias towards the one strong sample. Other mathematical operations besides the mean are also possible: median value or mode, for instance, which are less sensitive to outliers than the mean, or minimum or maximum values (“brightest return”), which specifically seek the outliers and can thus be useful for detecting targets.

Likewise, the management of overlapping lines is an operating choice with several options available and equally suitable. A common choice is to consider each sample contributing to a grid cell independently from its line of origin, which “blends” the lines together but has the perhaps undesirable consequence of averaging together data from different incidence angles or azimuth angles (orientation relative to North) or inhomogeneous levels of quality (e.g. in terms of signal-to-noise ratio). Another common method is to actively avoid blending adjacent lines by limiting cell calculations that involve data from more than one line to the samples belonging to one line only. The choice of which line to keep can then be made on the basis of which line is closest in horizontal distance from that specific cell, or which has the most appropriate angle of incidence, or signal-to-noise ratio. In this case, the drawback is that the final mosaic shows a visible “seam” between overlapping lines. A solution to the

conundrum is to use some weighting algorithm to operate a trade-off between the “blending” and “seaming” strategies, perhaps preferentially weighting those beam angles which provide the best discrimination and least noise (de Oliveira Junior and Hughes Clarke 2007).

The second step of mosaicking is the application of image enhancements algorithms (de-speckling, anti-aliasing, low-pass filtering, etc.) after the grid is complete. The possible techniques are the same as discussed at the stage of pre-mosaicking corrections. They are indeed more often applied at this stage in the two dimensions northing/easting since the grid is the final product, with the most common operation being the application of a noise-reduction low-pass filter such as a median filter.

The third step of mosaicking is the colour-scale mapping. It is the decision of how to map backscatter values in their current unit (dB or others) to the standard 8-bit scale (pixel values ranging between 0 and 255) or 16-bit scale (0 to 65,535) that greyscale images are usually coded in. This decision is often made subjectively by the operator for optimal visual interpretation. However, it is a critical choice that strongly impacts the aspect of the final mosaic, and a critical piece of information that is necessary to retrieve a dB level from a mosaic file, but that is very often completely overlooked. This choice includes the backscatter level bounds to “crop” the data to, and the data-unit-to-pixel-value mapping function (linear or otherwise). No standard exists for these choices although some values appear more obvious, such as not cropping the data (i.e. keeping minimum and maximum backscatter level), cropping at a factor of the standard deviation around the mean (the QPS FMGT software has the option to automatically crop to three times the standard deviation), or using set percentiles (i.e. 5 and 95% would probably be suitable in most cases). It is also common of operators to choose values to subjectively maximize contrast over the range of measured values, for a feature or area of interest. The mapping method of choice is to linearly map the value in dB to the pixel value, although the logarithmic nature of the dB scale implies that it would be just as valid an option to use a logarithmic mapping method instead. All this critical information can be summarized simply as a short annotation on backscatter maps or as part of its caption, for instance: “Data in dB units were [all kept/cropped at 5–95% percentiles/cropped at $\pm 3\sigma$ /cropped at $-X$ to $-Y$ dB], and mapped [linearly/logarithmically] to an [8/16]-bit scale”.

The fourth and final step of mosaicking is the choice of the color scale used to represent the data. The common practice is to use a grayscale color bar (i.e. shades of grey ranging from black to white), although it is not always the case (e.g. Hill et al. 2014). It is debatable whether low backscatter should be represented in black and high backscatter in white, as in Fig. 1a, or the other way around. The decision to represent increasing backscatter level in

increasingly bright tones is supported by the fact that higher reflectivity indicates higher energy, which translates for example in low-energy acoustic shadows in the lee of a significant feature on the seafloor to be shown dark as in our visual perception of the shadow of objects in the sunlight. The opposite decision to represent increasing backscatter level in increasingly dark tones is supported by the fact that (1) this follows the original convention of analogue sidescan sonars (which would print images on a thermal paper that darkens when exposed to heat), and that (2) rocks are more reflective than soft sediments and would therefore appear darker than sand on a sonar image, as on a regular photography, and help for interpretation. The choice is of little consequence and therefore left to the preference of the operator, but it must be clearly documented in a legend or metadata.

Conclusions and recommendations for backscatter data processing

In this article, we reviewed the backscatter data processing chain while highlighting the varied and complex ways in which backscatter data processing implementation can differ. While data decoding (stage 1), georeferencing (stage 2), and the radiometric corrections related to the hardware (CorGR and CorMP in stage 3) are constrained by the system and the sonar equation, the information necessary to operate these processing stages comes with considerably varied levels of availability and detail between sonar systems, sonar models, or modes of operation. In comparison, CorWS (stage 3), correction for angular dependence (stage 4), the pre-mosaicking corrections (stage 5) and the mosaicking methodology (stage 6) require little to no information, but present considerable freedom in software implementation. Reducing inconsistency in the future will therefore require agreeing on (1) the quantity and accuracy of the information that is necessary for the earlier processing stages, as well as (2) standard, documented procedures for the later stages.

These needs may be fulfilled by some form of standard coding of the various processing stages. Lamarche and Lurton (2017) suggested a possible coding, in the form of a nomenclature that categorizes the alternative approaches at each processing stage, thereby providing a framework metadata format for backscatter mosaics. While we fully support this nomenclature as such format would provide much-needed information to the user about their backscatter data products, it does not entice manufacturers and programmers to evolve towards more control in the backscatter data that sonar systems and software provide. A possible solution is presented here, namely a sequential terminology for increasingly refined levels of processing, modelled after the

approach adopted for satellite remote-sensing data (EOSDIS 1986, 2017), and following the processing sequence of this article

- BL_0 : The recorded level as it is currently recorded in data files. Most levels currently provided by existing systems can be considered BL_0 , which mostly indicates that the provided level is not controlled at this stage and that the users can expect levels from different systems to widely differ from one another.
- BL_1 : The level obtained after applying CorGR to BL_0 . Without the gains in reception, BL_1 should be the level of the received acoustic power directly after conversion from acoustic pressure by the hydrophones (in dB re. 1 V). The term “ BL_1 ” would indicate to its user that this “backscatter level” requires no more compensation for gains introduced in reception by the firmware, although other types of correction are still required for this level to be exploitable.
- BL_2 : The level obtained after applying the CorWS to BL_1 . Because the gains applied in reception are often rough corrections for Transmission Losses and insonified area, many current software consider the gains a “bad” CorWS, estimate a “better” one instead, compute the residuals between the two and compensate BL_0 for them. This one-step “CorGR + CorWS” correction readily brings the level from BL_0 to BL_2 , but we do encourage the use of the intermediate processing step BL_1 so as to stress the need for accurate documentation about gains from manufacturers. The term “ BL_2 ” would indicate to its users that this “backscatter level” is free of gains and dependence on range, and only dependent on the seafloor characteristics and the angle of transmission/reception, so that it is suitable for the extraction of beam patterns.
- BL_3 : The level obtained after applying CorMP to BL_2 . With an ideal correction, BL_3 should be the actual seafloor backscattering strength (in dB re $1 \text{ m}^2 \text{ per m}^2$)—free of hardware gains, calibration measurements, transmission losses and area of insonification, and only dependent on frequency, angle of incidence and seafloor type—and realistically the only term in the list deserving the initials “BS”. However, since the use of “BS” for uncalibrated level is still widespread, we do recommend the use of “ BL_3 ”. If acquired at a single frequency and segregated by angle of incidence β , $BL_3(\beta)$, is an angular response with *de facto* “absolute” level, that is, readily useable for angular response geophysical analyses.
- BL_4 : The level obtained after compensating BL_3 (that is, BS) for its dependence with angle of incidence, ready to be mosaicked. It can be debated whether BL_4 could be instead written with mentions to the reference angle in order to indicate that the level displayed is not the backscattering strength, but an “angle-corrected” version of

it. For example, one could write instead BS_{45° for a level referenced to an incident angle of 45° —as previously suggested by Lamarche et al. (2011)—or BS_{20-60° for a level referenced to the average level in the $20-60^\circ$ interval. Given that the value mapped is also dependent on frequency, this concept could be extended by mentioning the relevant frequency, for example: $BS_{45^\circ, 300\text{ kHz}}$ for an angle-corrected level referenced at 45° from a system that operated at 300 kHz.

Recommendations to sonar manufacturers

Some manufacturers such as Kongsberg Maritime and Teledyne Reson make good attempts at providing corrected backscatter data that follow most of what is called for in this document. For instance, the “Normalized Backscatter” feature introduced recently by Teledyne Reson (2015) was found to give very close results to what QPS FMGT produces from the raw beam time-series data. Similarly, Kongsberg Maritime refined its gains over time to reflect the advancements made in post-processing over the years. These recorded levels may very well be considered refined BL_3 or BL_4 . However, this does not mean that these recorded levels are ideal. As we saw, in many cases, the manufacturer corrections need to be removed to implement better processing algorithms and these “refined levels” then become a major obstacle.

Therefore, a case is to be made for manufacturers to provide backscatter data at earlier stages of processing, to allow flexibility in the subsequent data processing. A standard default backscatter level to output would ideally be BL_1 . In effect, by offering programmers a level free of all known gains in reception (constant and time-varying ones), manufacturers would eliminate a major part of the uncertainty in their radiometric corrections. Doing so would also have the additional interest for manufacturers to allow hiding any potentially commercially-sensitive approaches in hardware (e.g. time-varying gain), while providing a more controlled product. Until a manufacturer has sufficient knowledge and control of its gains to allow their own removal “on the fly”, they may instead output BL_0 and strive to provide information as accurate as possible for operators to remove these gains.

In addition to outputting BL_1 by default, manufacturers would ideally provide the parameters necessary for all subsequent corrections. The parameters necessary for CorWS (depth- and frequency-dependent absorption coefficients, effective pulse length or bandwidth, frequency-dependent beam widths) are often already provided. Ideally, this would be completed by parameters necessary for CorMP, that is, results of a calibration of each individual system along with the date of calibration. Failing so, at least generic values

for the corresponding model would be welcome. These values could be output in the data themselves for unambiguous retrieval (compared to a document, or personal communication, which rapidly gets outdated), perhaps in a dedicated “radiometric corrections” or “calibration” datagram. Methods could be created to allow operators to input new values (with new dates) in the acquisition software so that updated values are recorded along with new data files (even if they are not applied to the backscatter level BL_1 recorded in the raw data files).

Note that if manufacturers were to provide the necessary parameters to implement CorWS and CorMP, they would very well be able to implement their own versions of these corrections and therefore compute the subsequent levels BL_2 , BL_3 or BL_4 “on the fly” and record them in the data files. This would provide programmers and operators with a more refined product directly available from the raw data files, ready or almost ready to be mosaicked. In many respects, this is what Kongsberg Maritime does with its complex TVG, and Teledyne Reson with “Normalized Backscatter”. However, manufacturers should ensure to make BL_1 the default backscatter level provided so that programmers can always implement the superior algorithms that are often only possible in post processing thanks to the availability of, for instance, cleaned bathymetry maps (for CorWS), more recent calibration measurements (for CorMP), or new angular dependence correction algorithms.

Recommendations to software programmers

If manufacturers implement all, or some of, the recommendations above, programmers should liaise with them to ensure where in the data files to find BL_1 as well as the parameters (with clear definitions of their units) necessary for CorMP and CorWS. Programmers would then be able to design software that implement CorWS on BL_1 to retrieve BL_2 , CorMP on BL_2 to retrieve BL_3 and an angular dependence correction algorithm to produce some version of BL_4 .

Each of these levels should be exportable. BL_2 could then be used in input to software designed to extract new beam patterns, using calibration procedures established in partnership with manufacturers and researchers. BL_3 , exported along with the corresponding angle of incidence, would be angular response datasets, readily useable by researchers for angular response analysis.

Ideally, in the earlier stages of processing, software would allow the operator to override parameter values with new ones. This is particularly important for the CorMP parameters that may have been re-calculated through a new calibration, but also critical parameters of CorWS for which better values may have become available, such as a measurement of the effective pulse length or a more suitable coefficient of absorption. For the later stages of processing, the more

Detailed metadata for backscatter data products

- General:
 - System used: manufacturer, model, system serial number.
 - Parameters used in acquisition: operating frequency or frequencies (transmit sectors), “mode(s)” of operation (CW or FM pulse, etc.), dual head, transmit power and gain settings, etc.
- Stage 1. Raw data decoding:
 - Backscatter data type and units.
 - Process of calculation of this type and/or relevant datagram version.
- Stage 2. Georeferencing:
 - Information regarding how the XYZ positions of the samples were calculated (ideally, formulas).
 - Information regarding how the incidence angles of the samples were calculated (ideally, formulas).
- Stage 3A. Correction for the Gains applied in Reception (CorGR):
 - Were the built-in static and time-varying gains compensated for? What values/equations were used?
- Stage 3B. Correction for the effects of propagation through the Water-column and interaction with the Seafloor (CorWS):
 - What models of transmission losses were applied?
 - How was sound absorption considered: Constant value, depth-dependent, frequency dependent?
 - What model of insonified area was used?
- Stage 3B. Correction for the Mechanical Properties of the transducers (CorMP):
 - Was an absolute value used to correct for gains in the axis (source level, receive sensitivity) in bulk or separately measured? Provide values.
 - Were beam patterns compensated for? Provide values.
- Stage 4. Angle dependence removal:
 - Assuming the standard methodology was followed:
 - What was the data subset used for correction (e.g. one for all dataset, one per file, sliding window size, etc.)?
 - What operation was used to calculate the corrective curve from the subset (mean or median, linear units or dB, etc.)
 - What was the reference angle, or angular interval, used (if any)?
 - Was the standard deviation corrected as well?
 - If not, description of the methodology, or at least name of the proprietary algorithm and version.
- Stage 5. Pre-mosaicking corrections:
 - Any detail on pre-mosaic data filtering.
- Stage 6. Mosaicking:
 - Projection of final mosaic.
 - Step 1a: Grid resolution value.
 - Step 1b: Gridding strategy. How were the values blended in a one cell? What strategy for line overlap?
 - Step 2: Any post-mosaic image enhancement correction?
 - Step 3: Colour-scale mapping information (e.g. “Data in dB units were [all kept / cropped at 5%-95% percentiles / cropped at $\pm 3\sigma$ / cropped at -X to -Y dB], and mapped [linearly / logarithmically] to an [8 / 16]-bit scale”).

Fig. 6 Example of metadata information to be provided for each of the processing stages

parameters available, the better. Particularly, the angle (or angular interval) of reference in the angular dependence correction should be selectable.

For operators to fully understand their data products and make good use of them, it is imperative for them to have detailed information about the algorithms employed in their processing. To this end, programmers are encouraged to document fully (or as fully as commercial confidentiality allows) the steps taken in those backscatter data processing operations. In any case, the software should always output all processing parameters along with their output as a form of metadata, from the coefficient of absorption all the way to the color scale mapping utilized. Figure 6 presents the detail that could be included.

Recommendations to sonar operators

Ideally, operators would calibrate their systems regularly to produce the necessary parameters for accurate CorMP. However, it will be necessary to agree on feasible standard calibration procedures first, and to have software that allow input for these parameters.

Beyond this, it is incumbent on operators to ensure their data products have the required metadata regarding the data acquisition and subsequent processing to inform interpretation of the data products. This metadata shall be provided as a report, article or appendix to a dataset. Until programmers make this output standard, the operators will need to collect manually the necessary information, as per the nomenclature proposed by Lamarche and Lurton (2017) and/or the list suggested in Fig. 6.

References

- APL (1994) APL-UW high-frequency ocean environmental acoustic models handbook, Technical report 9407. Applied Physics Laboratory University of Washington, Seattle, WA
- APL (2000) High-frequency bistatic scattering model for elastic seafloors, Technical memorandum 2-00. Applied Physics Laboratory University of Washington, Seattle, WA
- Augustin J-M, Lurton X (2005) Image amplitude calibration and processing for seafloor mapping sonars. *Oceans 2005—Europe*, vol 1, pp 698–701
- Augustin J-M, Edy C, Savoye B, Le Drezen E (1994) Sonar mosaic computation from multibeam echo sounder. In: *OCEANS 94*, vol 2. ‘Oceans engineering for today’s technology and tomorrow’s preservation.’ Proceedings, p II/433–II/438
- Augustin J-M, Lamarche G, Lurton X, Pallentin A (2013) Sonar scope recent achievements in backscatter processing application to the reflectivity of The Brothers Area, NZ. QPS Workshop “Multibeam Backscatter State of the Technology, Tools & Techniques”, GeoHab Conference
- Beaudoin JD, Hughes Clarke JE, van den Ameerle EJ, Gardner JV (2002) Geometric and radiometric correction of multibeam backscatter derived from Reson 8101 systems. Canadian Hydrographic Conference 2002 Proceedings, Toronto, ON
- Beaudoin JD, Hughes Clarke JE, Bartlett JE (2004) Application of surface sound speed measurements in post-processing for multi-sector multibeam echosounders. *Int Hydrogr Rev* 5:26–31
- Carvalho RdC, Hughes Clarke JE (2012) Proper environmental reduction for attenuation in multi-sector sonars. In: Proceedings of the Canadian hydrographic conference, Niagara Falls, Ontario, Canada. pp 1–15
- Che Hasan R, Ierodiaconou D, Laurenson L (2012) Combining angular response classification and backscatter imagery segmentation for benthic biological habitat mapping. *Estuar Coastal Shelf Sci* 97:1–9. <https://doi.org/10.1016/j.ecss.2011.10.004>
- de Oliveira Junior AM, Hughes Clarke J (2007) Recovering wide angular sector multibeam backscatter to facilitate seafloor classification. U.S. Hydrographic Conference. Norfolk, VA, p 22
- De Moustier C, Kraft BJ (2013) In situ beam pattern estimation from seafloor acoustic backscatter measured with swath mapping sonars. In: Proceedings of Meetings on Acoustics ICA2013, vol 19, No. 1, p 070013
- De Falco G, Tonielli R, Di Martino G et al (2010) Relationships between multibeam backscatter, sediment grain size and *Posidonia oceanica* seagrass distribution. *Cont Shelf Res* 30:1941–1950. <https://doi.org/10.1016/j.csr.2010.09.006>
- Demer DA, Berger L, Bernasconi M et al (2015) Calibration of acoustic instruments. ICES Cooperative Research Report No. 326. p 133
- EOSDIS (1986) Report of the EOS data panel, vol IIa, NASA Technical Memo 87777
- EOSDIS (2017) EOSDIS Handbook—March 2017. https://cdn.earthdata.nasa.gov/conduit/upload/6321/EOSDIS_Handbook_1.3.pdf. Accessed 15 June 2017
- Fonseca L, Calder B (2005) Geocoder: an efficient backscatter map constructor. U.S. Hydrographic Conference, San Diego, CA
- Fonseca L, Mayer L (2007) Remote estimation of surficial seafloor properties through the application angular range analysis to multibeam sonar data. *Mar Geophys Res* 28:119–126
- Fonseca L, Calder B, Wetzler M (2006) Experiments for multibeam backscatter adjustments on the NOAA ship fairweather. In: *Oceans 2006*, vol 1–4, IEEE, New York, pp 323–326
- Fonseca L, Brown C, Calder B, Mayer L, Rzhanov Y (2009) Angular range analysis of acoustic themes from Stanton Banks Ireland: a link between visual interpretation and multibeam echosounder angular signatures. *Appl Acoust* 70:1298–1304
- Foote KG, Dezhong C, Hammar TR, Baldwin KC, Mayer LA, Hufnagle LC, Jech JM (2005) Protocols for calibrating multibeam sonar. *J Acoust Soc Am* 117:2013–2027. <https://doi.org/10.1121/1.1869073>
- Francois RE, Garrison GR (1982) Sound absorption based on ocean measurements: part II: boric acid contribution and equation for total absorption. *J Acoust Soc Am* 72:1879–1890
- Gavrilov AN, Duncan AJ, McCauley RD, Parnum IM, Penrose JD, Siwabessy PJW, Woods AJ, Tseng Y-T (2005) Characterization of the Seafloor in Australia’s Coastal Zone using acoustic techniques. Proceedings of the international conference ‘underwater acoustic measurements: technologies and results’, Crete, Greece
- Hammerstad E (2000) EM technical note, backscattering and seabed image reflectivity. p 5
- Hammerstad E (2005) EM technical note, sound levels from Kongsberg multibeam. p 3
- Heaton JL, Rice G, Weber TC (2017) An extended surface target for high-frequency multibeam echo sounder calibration. *J Acoust Soc Am* 141:EL388–EL394. <https://doi.org/10.1121/1.4980006>
- Hellequin L, Lurton X, Augustin J-M (1997) Postprocessing and signal corrections for multibeam echosounder images. In: *OCEANS’97*, vol 1. MTS/IEEE Conference Proceedings. pp 23–26

- Hill NA, Lucieer V, Barrett NS, Anderson TJ, Williams SB (2014) Filling the gaps: predicting the distribution of temperate reef biota using high resolution biological and acoustic data. *Estuar Coastal Shelf Sci* 147:137–147
- Hiroji AD, Hughes Clarke JE (2017) Radiometric compensation strategy for multispectral backscatter data. In: U.S. Hydrographic Conference. Galveston, Texas, USA
- Hiroji AD, Hughes Clarke JE (2016) Multi-sector radiometric beam pattern extraction method for improved seafloor classification. In: Canadian hydrographic conference 2016. Halifax, NS, Canada, pp 1–21
- Huang Z, Siwabessy J, Nichol S, Anderson T, Brooke B (2013) Predictive mapping of seabed cover types using angular response curves of multibeam backscatter data: Testing different feature analysis approaches. *Cont Shelf Res* 61–62:12–22. <https://doi.org/10.1016/j.csr.2013.04.024>
- Hughes Clarke J (1994) Toward remote seafloor classification Using the angular response of acoustic backscattering: a case study from multiple overlapping GLORIA data. *IEEE J Ocean Eng* 19:112–127
- Hughes Clarke JE (2012) Optimal use of multibeam technology in the study of shelf morphodynamics. *Int Assoc Sedimentol Spec Publ* 44:3–28
- Hughes Clarke JE (2015) Multispectral acoustic backscatter from multibeam, improved classification potential. U.S. Hydrographic Conference. p 19
- Hughes Clarke J, Danforth BW, Valentine P (1997) Areal seabed classification using backscatter angular response at 95 kHz. High frequency acoustics in shallow water, Lerici, Italy
- Hughes Clarke JE, Iwanowska KK, Parrott R et al (2008) Inter-calibrating multi-source, multi-platform backscatter data sets to assist in compiling regional sediment type maps: Bay of Fundy. In: Canadian hydrographic conference national surveyors conference 2008. Victoria, BC, Canada, p 22
- Kloser RJ, Penrose JD, Butler AJ (2010) Multi-beam backscatter measurements used to infer seabed habitats. *Cont Shelf Res* 30:1772–1782. <https://doi.org/10.1016/j.csr.2010.08.004>
- Lamarche G, Lurton X (2017) Recommendations for improved and coherent acquisition and processing of backscatter data from seafloor-mapping sonars. *Mar Geophys Res*. <https://doi.org/10.1007/s11001-017-9315-6>
- Lamarche G, Lurton X, Verdier A-L, Augustin J-M (2011) Quantitative characterisation of seafloor substrate and bedforms using advanced processing of multibeam backscatter—application to Cook Strait, New Zealand. *Cont Shelf Res* 31:S93–S109
- Lanzoni C, Weber T (2011) A method for field calibration of a multibeam echo sounder. *Oceans* 2011, p 7
- Le Bas TP, Huvenne VAI (2008) Acquisition and processing of backscatter data for habitat mapping—comparison of multibeam and sidescan systems. *Appl Acoust* 70: 1248–1257. <https://doi.org/10.1016/j.apacoust.2008.07.010>
- Le Gonidec Y, Lamarche G, Wright IC (2003) Inhomogeneous substrate analysis using EM300 backscatter imagery. *Mar Geophys Res* 24:311–327. <https://doi.org/10.1007/s11001-004-1945-9>
- Leblanc E, Foster B (2015) New algorithm for multibeam imagery processing. Marine technology reporter white papers, hydrographic edition, pp 40–44
- Lucieer V, Roche M, Degrendele K, Malik M, Dolan M, Lamarche G (2017) User expectations for multibeam echo sounders backscatter strength data—looking back into the future. *Mar Geophys Res*. <https://doi.org/10.1007/s11001-017-9316-5>
- Lurton X (2010) An introduction to underwater acoustics—principles and applications, 2nd edn. Springer-Verlag, Berlin. p 680
- Lurton X, Lamarche G (2015) Backscatter measurements by seafloor mapping sonars: guidelines and recommendations. <http://geoahb.org/wp-content/uploads/2013/02/BWSG-REPORT-MAY2015.pdf>. Accessed 15 June 2017
- MacLennan DN, Fernandes PG, Dalen J (2002) A consistent approach to definitions and symbols in fisheries acoustics. *ICES J Mar Sci* 59:365–369. <https://doi.org/10.1006/jmsc.2001.1158>
- Melvin GD, Cochrane NA, Li Y (2003) Extraction and comparison of acoustic backscatter from a calibrated multi- and single-beam sonar. *ICES J Mar Sci* 60:669–677. [https://doi.org/10.1016/S1054-3139\(03\)00055-9](https://doi.org/10.1016/S1054-3139(03)00055-9)
- Parnum IM (2007) Benthic habitat mapping using multibeam sonar systems. PhD Thesis, Curtin University
- Parnum IM, Gavrilov A (2011a) High-frequency multibeam echosounder measurements of seafloor backscatter in shallow water: part 1—data acquisition and processing. *Underwater Technol* 30:3–12
- Parnum IM, Gavrilov A (2011b) High-frequency multibeam echosounder measurements of seafloor backscatter in shallow water: part 2—mosaic production, analysis and classification. *Underwater Technol* 30:13–26
- Parnum IM, Gavrilov AN, Siwabessy PJW, Duncan AJ (2006). Analysis of high-frequency multibeam backscatter statistics from different seafloor habitats. Eighth European conference on underwater acoustics, 8th ECUA, Carvoeiro, Portugal. p 6
- Preston JM (2009) Automated acoustic seabed classification of multibeam images of Stanton Banks. *Appl Acoust* 70:1277–1287
- QPS (2017) Beam Pattern Correction, pp 296–297. In: Fledermaus v7.7.x Manual. p 562
- Rice G, Greenaway SF, Weber TC, Beaudoin J (2012) Methods for collecting and using backscatter field calibration information for the Reson 7000 Series Multibeams. In: Canadian hydrographic conference 2012
- Schimel ACG, Healy TR, McComb P, Immenga D (2010) Comparison of a self-processed EM3000 multibeam echosounder dataset with a QTC view habitat mapping and a sidescan sonar imagery, Tamaki Strait, New Zealand. *J Coastal Res* 26:714–725
- Schimel ACG, Beaudoin J, Gaillot A, Keith G, Le Bas T, Parnum I, Schmidt V (2015) Chapter 6: Processing Backscatter Data: From Datagrams to Angular Response and Mosaics. In: Lurton X, Lamarche G (eds) Backscatter measurements by seafloor-mapping sonars. Guidelines and Recommendations. p 200
- Tamsett D, Hogarth P (2016) Sidescan sonar beam function and seabed backscatter functions from trace amplitude and vehicle roll data. *IEEE J Ocean Eng* 41:155–163. <https://doi.org/10.1109/JOE.2015.2390732>
- Teledyne Reson (2015) SeaBat T50-P product description. p 22
- Urick RJ (1983) Principles of underwater sound, 3rd edn. McGraw-Hill, New York. p 444